The Effect of Surface Active Agents on Interphase Mass Transfer

J. C. BURNETT, JR., and D. M. HIMMELBLAU

The University of Texas, Austin, Texas

The effect of various soluble and insoluble surface active agents on the absorption of ammonia into a static aqueous system was studied. Saturated straight-chain hydrocarbons with four to twenty-two carbon atoms and polar end groups were selected as the surface active agents to be studied. Alcohol, amine, and amide end groups were investigated. Most of the insoluble surface active agents, which were studied as films, were found to decrease the ammonia absorption rate. There was a definite correlation between the amount of mass transfer reduction and the hydrocarbon chain length, while the effect of the various end groups appeared to depend on the chain length. Surface mass transfer coefficients were computed for each surface active agent that retarded mass transfer. Most of the soluble surface active agents were found to increase the ammonia absorption rates. For all cases of enhanced mass transfer, movements in the interface could be observed. It was concluded that the interfacial movements were caused by the Marangoni effect. In general, as the chain length of the surface active agent decreased, the mass transfer enhancement increased. A mathematical model based on a surface renewal theory was fitted to the experimental data.

The effect that surface active agents have on interphase mass transfer is of interest for two main reasons. First, most commercial process liquids inadvertently contain surface active agents, which may drastically affect the mass transfer rates in distillation towers, absorbers, etc. (*12*). Second, insoluble surface active agents have been used for several years to retard the evaporation of water from reservoirs, a practice of considerable value in arid climates (*30*).

It has been generally concluded that the addition of a surface active agent to a system reduces the interphase mass transfer per unit area for that system. Two mechanisms have been proposed to explain the reduction, the hydrodynamic mechanism and the barrier mechanism. The hydrodynamic mechanism postulates that surface active agents alter the hydrodynamics of a flow system and that this alteration is the prime cause of mass transfer reduction. The barrier mechanism proposes that surface active agents physically block interphase mass transfer in addition to exhibiting the hydrodynamic effect.

Both static and flowing fluids have been employed to study the effect of monolayers in interphase gas transfer. Relatively few investigators have studied static gas-liquid systems. This method, in principle, would appear to be an excellent one to detect any barrier mechanism of mass transfer reduction, since hydrodynamic factors are excluded. Blank and Roughton (*5*) and Blank (*4*) investigated the effect of insoluble monolayers on the absorption of several gases by water or chemically reactive solutions and reported that no convective instability developed during the contact times they used. Several insoluble monolayers were found to be effective in retarding mass transfer, while a few films had no effect.

Hawke (*24*), Hawke and Parts (*26*), Hawke and Alexander (*25*), Hawke and White (*27*), and Hawke and Wright (*28*) allowed radioactive H_2S^{35} and $C^{14}O_2$ to diffuse out of a static water layer which was covered with an insoluble monolayer, and mass transfer rates were determined by radioactive counting techniques. Stable mass transfer took place for all times. The authors found that some monolayers retarded mass transfer, while others had no effect. Harvey and Smith (*23*) used an interferometric technique to measure liquid-phase concentrations as carbon dioxide absorbed into a static water phase. The soluble surface active agents Lissapol-N and Teepol were found to decrease the mass transfer rate for this system. Very short contact times were considered, so that convective instability was avoided.

Sada and Himmelblau (*37*) measured the effect of several insoluble monolayers on the desorption of gases from a static water phase. The use of desorption techniques provided stable mass transfer for all times. Mass transfer rates were found to be reduced by as much as 40% at high surface pressures.

The most recent work on static gas-liquid systems is that of Plevan (*35*), who measured the effect of several insoluble monolayers on the absorption of sulfur dioxide by water. Stable mass transfer took place for the first several seconds, after which convective instability became pronounced. The author measured a barrier type of mass transfer reduction during the first part of the experiment and the combined barrier plus hydrodynamic type of reduction for the remainder of the experiment.

Numerous flow systems have been used to study the effects of surface active agents in gas-liquid systems. The conclusions drawn from the use of a stirred liquid phase (*1, 17, 20, 31*) are that any barrier type of mass transfer reduction is confounded with the hydrodynamic effects. Laminar liquid jets (*15, 36, 40*) and falling liquid films (*14, 19, 29, 32, 34*) have produced results with varying interpretations as to the existence and extent of a barrier type of mechanism of reduction. Perhaps the most complicated flow regime for studying surface active agents is that of gas bubbles in a liquid phase (*3, 9, 18, 21, 33, 39, 41, 42*). Experiments analogous to those for gas-liquid systems have also been performed for liquid-liquid systems, including stirred liquid phases, laminar liquid jets, liquid

J. C. Burnett, Jr., is at Monsanto Company, Pensacola, Florida.

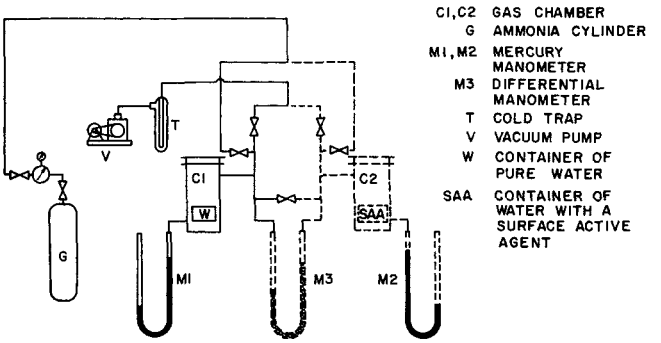

Fig. 1. Experimental apparatus (equipment in dashed lines used for differential absorption measurement).

drops in a contiguous liquid phase, and two static liquid phases. But, in general, the conclusions drawn from these studies as to the extent of a barrier type of reduction are indeterminate.

It was desired to study the effect of surface active agents on interphase mass transfer in a static gas-liquid system which was free of convective instabilities for all contact times. With such a system, insight could be gained into the barrier mechanism of mass transfer reduction for both soluble and insoluble surface active agents. Mathematical models would then be formulated to describe the experimental results.

MASS TRANSFER SYSTEM

A static water phase was selected to study the effect of surface active agents on mass transfer because a constant surface concentration of surface active agent could be maintained throughout an experiment, both insoluble and soluble surface active agents could be studied, and no hydrodynamic factors would be present to confuse the evaluation of the barrier mechanism of mass transfer reduction.

Ammonia gas was selected as the gas phase for two main reasons. First, ammonia is very soluble in water; therefore, high rates of mass transfer could be expected. The most important reason for the selection of ammonia arose from hydrodynamic stability considerations, however. Ammonia has the desirable property that ammonia solutions in water become less dense as the ammonia concentration increases. Therefore, as ammonia absorbs into water and the solution near the interface becomes more concentrated in ammonia than in the bulk, the liquid near the interface becomes less dense than the underlying liquid, and there is no tendency for convection currents to be set up because of density differences, as will occur with carbon dioxide and most other gases.

A constant volume technique in which the system was closed with respect to volume and the pressure of the chamber measured as it decreases with time was selected for the study because it was the easiest to execute experimentally.

Figure 1 presents the equipment diagram. The cylindrical gas chamber C1 was constructed of 5-in. stainless steel pipe.

A volume of 250 cc. of water was placed in a cylindrical polyethylene dish so as to fill the dish to within ⅛ in. of its top. Polyethylene was used in order to prevent condensation of water vapor on the exterior container surface. Water condensate would absorb ammonia, causing erroneous determinations of mass transfer rates to be made. In order to prevent condensation on the gas chamber and sight glass, they were heated prior to an experimental run

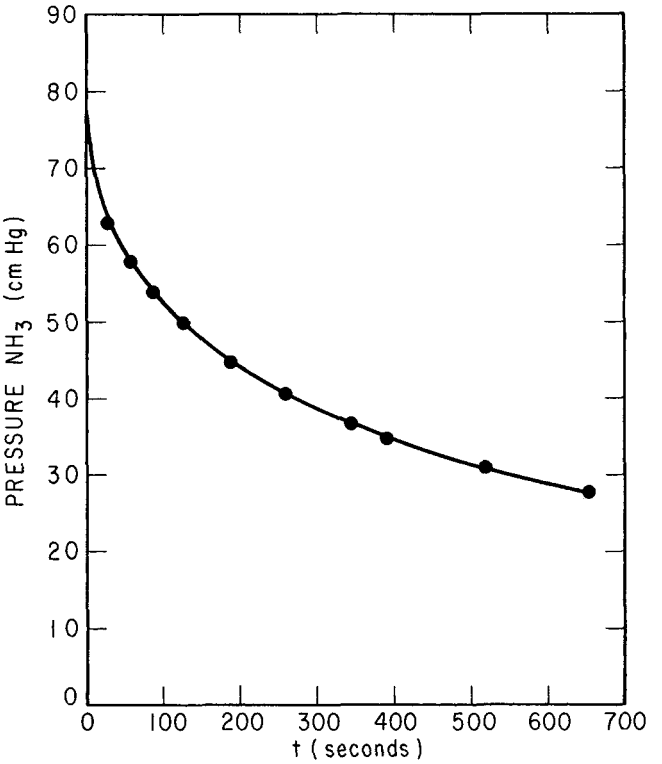

Fig. 2. Typical absorption curve run number 1. Original water temperature = 25.5°C.

to approximately 3°C. above room temperature.

Water for use in the mass transfer experiments was initially degassed by pulling a vacuum on the liquid while stirring it with a Teflon coated magnetic stirring bar. After degassing, the water was placed under vacuum in a constant temperature bath maintained at 25.5°C.

PROCESS MODEL

From the microscopic transport phenomena viewpoint, diffusion takes place in the two phases and across the interface. The microscopic equations of change must be written for the two phases and the interfacial condition given as a boundary condition to describe the mass transfer system properly. A commonly used interfacial boundary condition in the microscopic description is that equilibrium exists at the interfacial boundary. Equilibrium at the interface is equivalent to having no interfacial resistance. Under the usually encountered conditions, it is generally concluded that equilibrium exists at the interface of liquid-gas systems that contain no surface active agents (*23*).

The mathematical model for the mass transfer of ammonia into pure water is the ammonia mass balance written for the aqueous phase. A gas-phase ammonia balance is not needed, since no concentration gradients are present in the gas phase because no inert gases are present except the small amount of water vapor in equilibrium with the water phase.

It can be calculated that the reaction of ammonia with water is negligibly small, and it is assumed that the only pertinent diffusion is that perpendicular to the liquid-gas interface.

As ammonia diffuses into the liquid phase, the liquid expands slightly and the interface moves vertically upward, causing the location of the interface to vary with time. Hartley and Crank (*13, 22*) have introduced a coordinate system which was found to be very useful in describing this type of moving boundary problem. A new

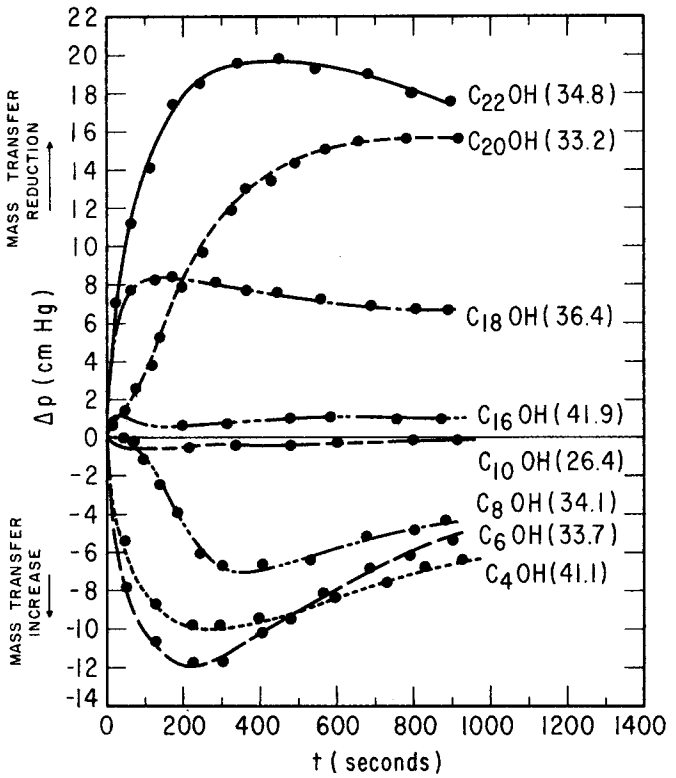

Fig. 3. Experimental data for C_{22}, C_{20}, C_{18}, C_{16}, C_{10}, C_8, C_6, and C_4. Alcohols at 25.5°C. (Surface pressure in dynes/cm. in parentheses.)

coordinate ξ is defined such that equal increments of ξ contain equal amounts of water. The new coordinate system expands with the swelling liquid phase such that each particle of water has the same coordinate at all times during the transfer. Therefore, the velocity of the water in the ξ coordinate system is zero.

In the ξ coordinate system

$$\frac{\partial C^B}{\partial t} = \frac{\partial}{\partial \xi}\left[\left(\frac{C^B}{C^W} + 1\right) D^B \frac{\partial C^B}{\partial \xi}\right] \tag{1}$$

Details of the derivation can be found in references *6*, *13*, and *22*.

An effective diffusion coefficient is defined by

$$D^E = \left(\frac{C^B}{C^W} + 1\right) D^B \tag{2}$$

and is assumed to be a constant. The value of (C^B/C^W) varied from 0 to 0.45 in this experimental work; however, an analytical solution is precluded unless D^E is assumed to be constant.

The mass balance assumes the well-known form

$$\frac{\partial C^B}{\partial t} = D^E \frac{\partial^2 C^B}{\partial \xi^2} \tag{3}$$

and the boundary and initial conditions are

Initial condition:

$$C^B = C_0, \quad \xi > 0, \quad t = 0 \tag{4a}$$

Boundary condition 1:

$$C^B = C_0, \quad \xi \to \infty, \quad t > 0 \tag{4b}$$

Boundary condition 2:

$$C^B = C^* + H_1 p + H_2 p^2, \quad \xi = 0, \quad t > 0 \tag{4c}$$

Gas-phase mass balance:

$$V\delta \frac{dp}{dt} = D^E A \left(\frac{\partial C^B}{\partial \xi}\right)_{\xi=0} \tag{5a}$$

Initial condition:

$$p = p_0, \quad t = 0 \tag{5b}$$

The initial condition, Equation (*4a*), specifies a uniform initial concentration of ammonia in the liquid, C_0. For this study, C_0 was equal to zero. Boundary condition 1 given by Equation (*4b*) is the usual semi-infinite boundary condition, which means that the depth of penetration of the solute is less than the liquid depth. The interfacial boundary condition, Equation (*4c*), specifies that the interfacial liquid is in equilibrium with the ammonia at pressure p at all times. In the range of gas pressures of 15 and 80 cm. Hg, the concentration of aqueous ammonia and the ammonia gas pressure does not obey Henry's law. As a result, a nonlinear relation, Equation (*4c*), is required for the interfacial boundary condition to represent the equilibrium properly. The interphase mass balance, Equation (*5a*), equates the instantaneous change in the amount of ammonia in the gas phase to the instantaneous interfacial flux of ammonia into the liquid phase. Thus, the gas-phase pressure is given as a function of time. Burrows and Preece (*7*) have used an interphase mass balance similar to Equation (*5a*) to describe constant volume mass transfer.

The technique used to solve the mathematical model is a modification of the series solution method of solving ordinary differential equations. It was realized that a solution to the component mass balance, Equation (3), subject to conditions of Equation (4) could be obtained if the right-hand side of Equation (*4c*) were only a function of the independent variable t. To force boundary condition 2 into this form, it was assumed that the pressure could be expressed as a power series in $t^{1/2}$ which converged in some region $0 \leq t \leq T$:

$$p = \sum_{j=0}^{\infty} a_j t^{j/2} \tag{6}$$

The coefficients a_j are specified by Equations (7) to (10).

The series solution technique proved to be successful,

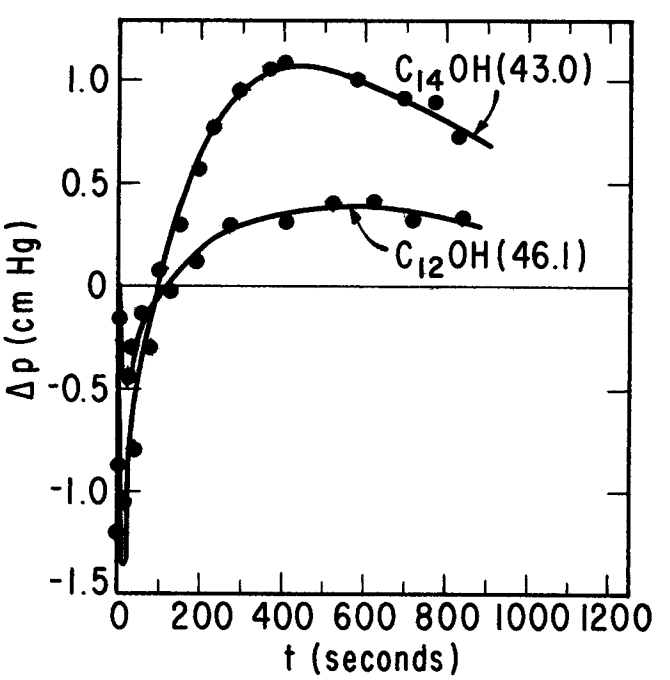

Fig. 4. Experimental data for C_{14} and C_{12} alcohol at 25.5°C. (Surface pressure in dynes/cm. in parentheses.)

and the solution of the mathematical model given by Equations (3), (4), and (5) was determined to be (6)

$$C^B = C_0 - \frac{H_1}{K\sqrt{D^E}} \sum_{j=1}^{\infty} a_j \Gamma\left(\frac{j+2}{2}\right) (4t)^{\frac{j-1}{2}} \left[i^{j-1}\,\mathrm{erfc}\left(\frac{\xi}{2\sqrt{D^E t}}\right)\right] \quad (7)$$

$$p = \sum_{j=0}^{\infty} a_j t^{j/2} \quad (8)$$

The recursion relationship between the coefficients is given below:

$$a_0 = p_0 \quad (9a)$$

$$a_1 = -\frac{\Gamma(1)}{\Gamma\left(\frac{3}{2}\right)} \frac{K\sqrt{D^E}}{H_1} [C^* + H_1 a_0 + H_2 a_0^2 - C_0] \quad (9b)$$

$$a_j = -\frac{\Gamma\left(\frac{j+1}{2}\right)}{\Gamma\left(\frac{j+2}{2}\right)} \frac{K\sqrt{D^E}}{H_1} \left[H_1 a_{j-1} + H_2 \sum_{\substack{k=0 \\ k+m=j-1}}^{j-1} \sum_{m=0}^{j-1} a_k a_m \right] \quad \text{for } j \geq 2 \quad (9c)$$

where

$$\sum_{\substack{k=0 \\ k+m=j-1}}^{j-1} \sum_{m=0}^{j-1} a_k a_m = a_0 a_{j-1} + a_1 a_{j-2} + a_2 a_{j-3} + \ldots$$

$$a_{j-3} a_2 + a_{j-2} a_1 + a_{j-1} a_0 \quad (9d)$$

The notation $i^n\mathrm{erfc}(u)$ is used to indicate a particular function, the n^{th} repeated integral of the error function (8).

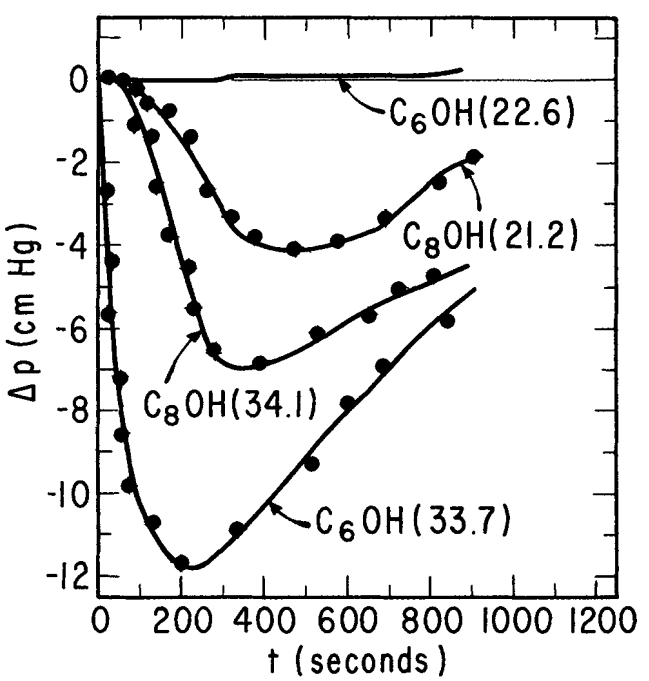

Fig. 5. Experimental data for C_8 and C_6 alcohol at 25.5°C. (Surface pressure in dynes/cm. in parentheses.)

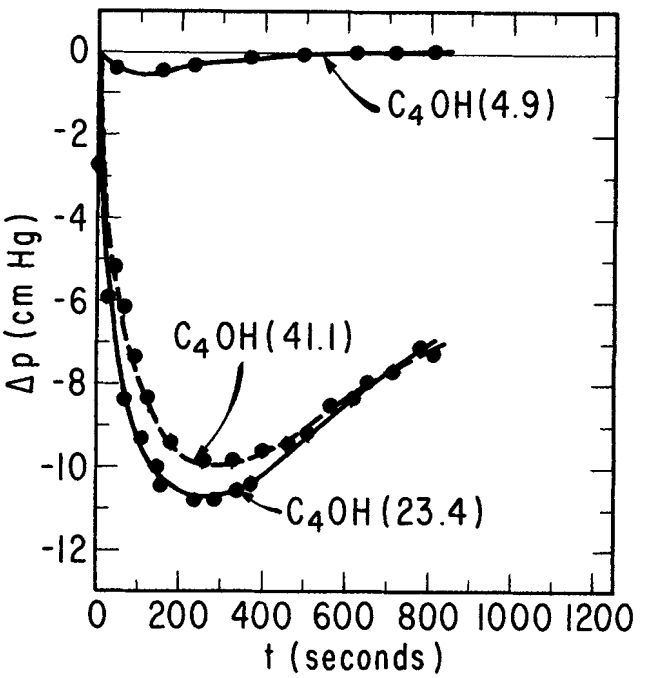

Fig. 6. Experimental data for C_4 alcohol at 25.5°C. (Surface pressure in dynes/cm. in parentheses.)

EXPERIMENTAL RESULTS FOR ABSORPTION WITHOUT SURFACE ACTIVE AGENTS

Two parameters, p_0 and D^E of Equations (8) and (9), were determined by a statistical fit of the experimental data. The values of p_0 and D^E which minimized the criterion S_p were selected as the best values of those parameters, where

$$S_p \equiv \sqrt{\frac{\sum_{i=1}^{N} \left[\frac{(p_{\text{exp}})_i - (p_{\text{calc}})_i}{(p_{\text{calc}})_i} (100) \right]^2}{(N-1)}} \quad (10)$$

The minimization was carried out on a digital computer employing the Hooke and Jeeves direct search procedures as modified by Anthony and Himmelblau (2).

Figure 2 presents the results of an absorption experiment in which the fitted parameters p_0 and D^E were determined to be 79.8 cm. Hg and 1.23×10^{-5} sq.cm./sec., respectively. The average value of the effective diffusion coefficient D^E determined from twenty-two experiments at 25.5°C. was 1.27×10^{-5} sq.cm./sec. with a standard deviation of 3.3×10^{-7}.

Using an infrared technique, Chiang (10) measured the surface temperature of a laminar water jet as it absorbed ammonia at pressures of 1 atm. It was found that the surface temperature rose to a maximum of 22°F. higher than the original bulk temperature. A large temperature effect was to be expected during the absorption of ammonia by water, since a large quantity of ammonia dissolves in the water phase releasing its heat of solution. Suppose it is assumed, as in the work of Chiang and Toor (11), that the surface temperature of the static water phase was constant with time but at a higher value than the initial bulk temperature. This assumption alters only one part of the mathematical model, namely, the equilibrium relation between the surface liquid and the pressure of ammonia, which would be different at a higher temperature. Thus, all that needed to be done to correct the model for the temperature effect was to change the constants C^*, H_1, and H_2 to the appropriate values. By using the equilibrium

relationship at 100°F. and the data in Figure 2, it was found that the fitted parameters p_0 and D^E had the values 80.9 cm. Hg and 2.37 × 10^{-5} sq.cm./sec., respectively. Chiang and Toor (*11*) report the diffusion coefficient in the x coordinate system D for ammonia transport into water to have the value 3.55 × 10^{-5} sq.cm./sec. at 104°F. The difference in magnitude of the two diffusion coefficients can be explained as follows. Hartley and Crank (*13, 22*) report the relationship between the diffusion coefficient in the x coordinate system D and the diffusion coefficient in the ξ coordinate system D^B to be

$$D^B = D\,(C^V\ V_W) \qquad (11a)$$

A combination of Equations (2) and (11*a*) gives the relationship between D and the effective diffusion coefficient D^E:

$$\frac{D^E}{D} = \left(\frac{C^B}{C^W} + 1\right)(C^V\ V_W)^2 \qquad (11b)$$

The average ammonia partial pressure in Figure 2 was 43 cm. Hg and use of the values of C^B, C^W, C^V, and V_W corresponding to this pressure at 100°F. yielded a value of (D^E/D) of 0.65 as compared with the value of (2.37 × 10^{-5}/3.55 × 10^{-5}) or 0.67 calculated from experimental diffusion coefficients. Thus, Equation (11*b*) describes the relation between D^E and D.

It was found that no improvement in the statistical fit of the data was obtained by assuming the surface temperature to be 100°F. instead of 78°F. Consequently, the solution to the isothermal mathematical model, Equation (8), with an interfacial temperature of 78°F. was used in all subsequent calculations for three reasons. First, the isothermal mathematical model at a surface temperature of 78°F. converged for longer contact times than the model at a surface temperature of 100°F. Second, since the surface temperature of the water surface was never measured, the selection of a surface temperature would be arbitrary. Third, the purpose of this study was not to measure the diffusivity of ammonia in water. Rather, the purpose was to detect any change in the absorption of ammonia by water when surface active agents were added to the water phase. Therefore, the solution of the isothermal model at a surface temperature of 78°F., even though it had limitations, was adequate for the purposes of this study.

MASS TRANSFER TO WATER CONTAINING A SURFACE ACTIVE AGENT

Saturated straight-chain hydrocarbons of four to twenty-two carbon atoms with polar end groups were selected as the surface active agents to be studied. Three end groups were chosen to be investigated: alcohols, amines, and amides.

Since previous investigators had shown that the effect of some surface active agents on mass transfer was quite small, it was desirable to construct a differential pressure experimental apparatus which could measure such small effects. The apparatus is shown in Figure 1, with the second cell and auxiliaries shown in dashed lines. The cells were interconnected by a differential manometer. In order to insure that both cells were of equal volume, blank runs were made in which pure water was placed in each compartment. Simultaneous mass transfer experiments were carried out with one container holding water with a surface active agent and the other free of surface active agent.

The surface active agent was added to the water in one of three ways.

1. Measured quantities of the soluble surface active agents (*n*-decyl alcohol, *n*-octyl alcohol, *n*-hexyl alcohol, *n*-butyl alcohol, *n*-decylamine, *n*-hexylamine, and hexanamide) were dissolved in the water.
2. Two of the surface active agents, *n*-dodecyl alcohol and *n*-tetradecyl alcohol, spread to quite large surface pressures when the pure alcohol was added to a water interface. These compounds were placed on the water substrate by adding several milligrams of the alcohol to the water surface.
3. The remaining surface active agents (*n*-docosyl al-

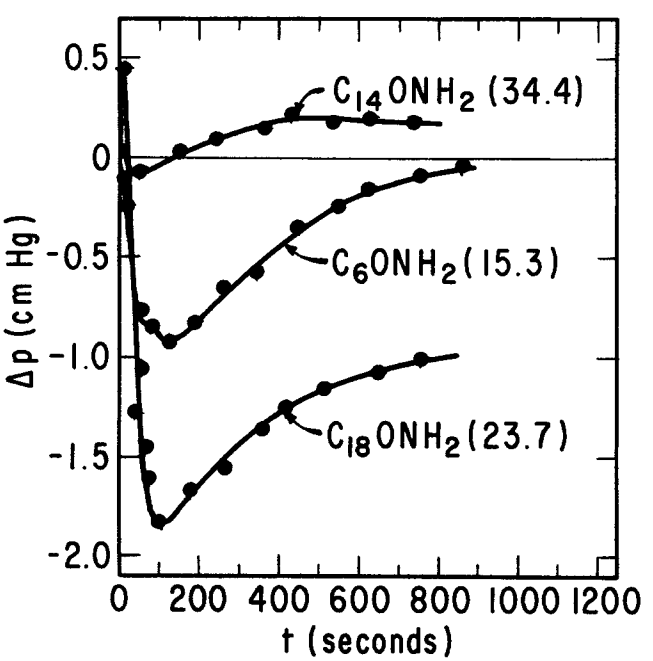

Fig. 7. Experimental data for C_{18}, C_{14}, and C_6 amide at 25.5°C. (Surface pressure in dynes/cm. in parentheses.)

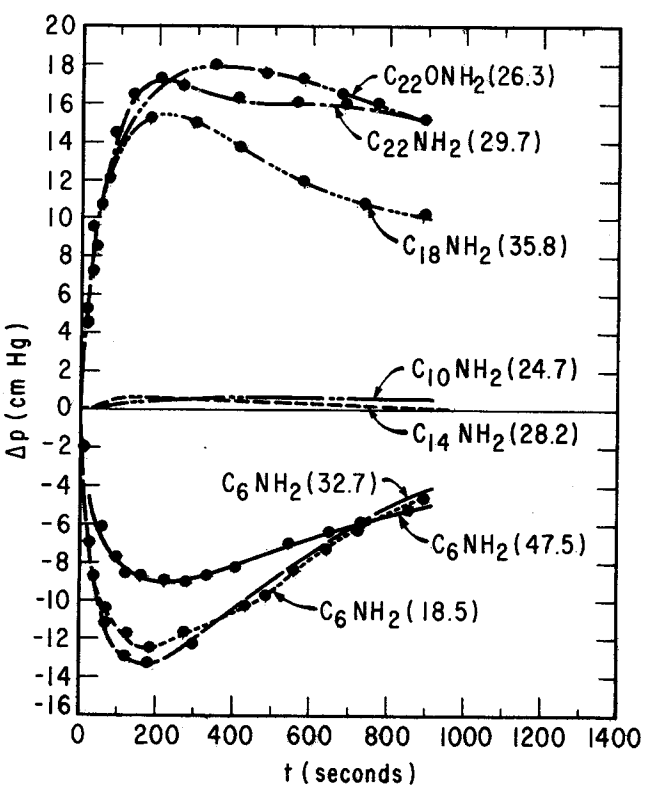

Fig. 8. Experimental data for C_{22} amide, C_{22}, C_{18}, C_{14}, C_{10}, and C_6 amine at 25.5°C. (Surface pressure in dynes/cm. in parentheses.)

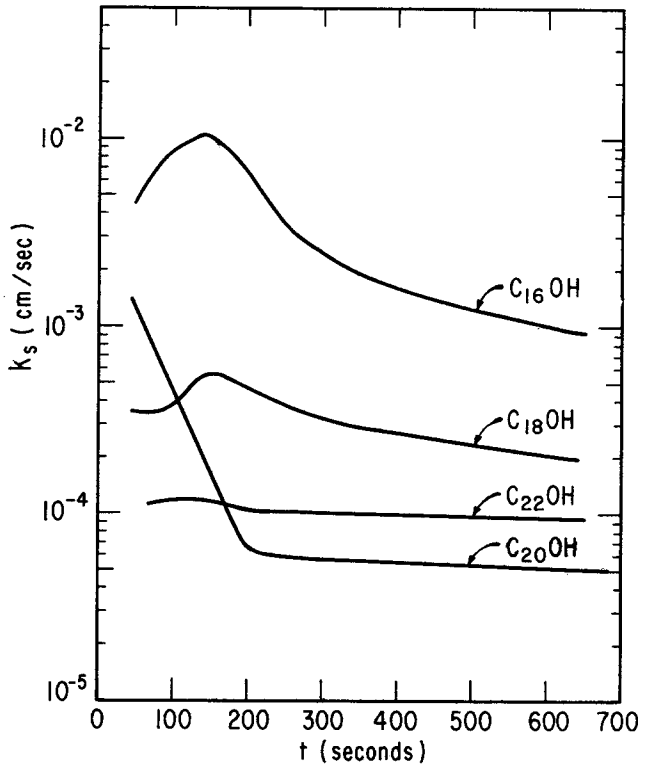

Fig. 9. Surface mass transfer coefficient vs. time for C_{22}, C_{20}, C_{18}, and C_{16} alcohol.

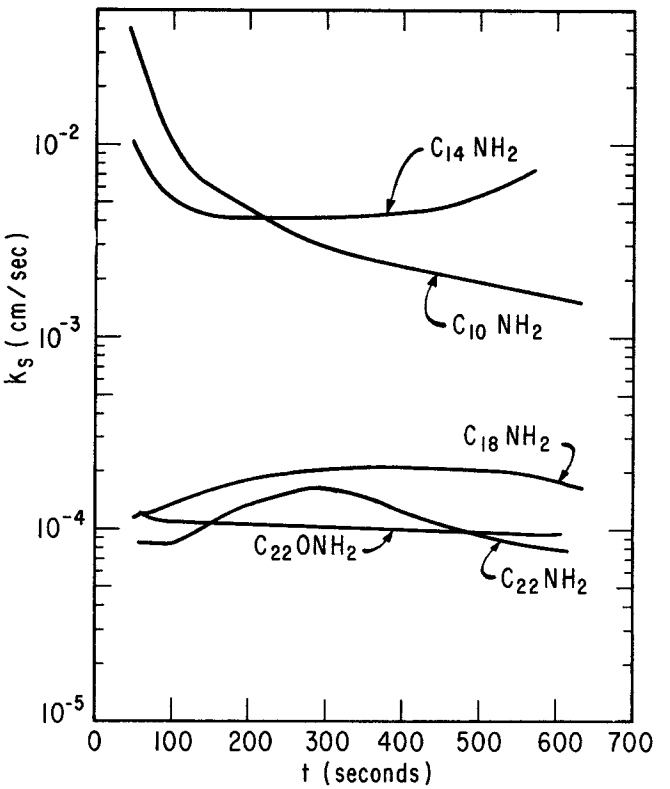

Fig. 10. Surface mass transfer coefficient vs. time for C_{22} amide, C_{22}, C_{18}, C_{14}, and C_{10} amine.

cohol, *n*-eicosyl alcohol, *n*-octadecyl alcohol, *n*-hexadecyl alcohol, *n*-docosylamine, *n*-octadecylamine, *n*-tetradecylamine, docosanamide, octadecanamide, and tetradecanamide) were handled as follows. A few milligrams of the solid material were added to the water surface. Then, approximately 0.04 cc. of approximately 0.1 wt. % ether solution of the surface active material was added to the surface. The amides would not dissolve in the ether solvent; hence, they were first dissolved in chloroform, and then one part of the chloroform solution was dissolved in four parts of ether solvent. Enough surface active material was added to the interface so that a surface excess could be observed throughout the absorption run.

The experimental results are presented in Figures 3, 4, 5, 6, 7, and 8 in the form of graphs of the differential pressure vs. the contact time t. The differential pressure is defined as the pressure in the compartment with the surface active agent p_{SAA} minus the pressure in the compartment with pure water p_W:

$$\Delta p = p_{SAA} - p_W \tag{12}$$

Two distinctly different types of behavior are demonstrated, namely, surface active agents that had a positive Δp for all contact times and agents that had a negative Δp for all contact times. The surface active agents that had a positive Δp retarded the mass transfer of ammonia into water. Conversely, those that had a negative Δp increased the mass transfer of ammonia into water.

For all experimental runs in which differential mass transfer rates were increased, movement at the interface could be detected. Conversely, no interfacial movement could be detected for the absorption of ammonia into pure water or into water containing the surface active agents which decreased mass transfer rates.

Figure 3 shows that the twenty-two to sixteen carbon atom alcohols decreased the mass transfer rate, with the magnitude of the reduction decreasing with decreasing chain length. Conversely, the ten to four carbon atom alcohols increased the mass transfer rate, with the magnitude of the enhancement increasing with decreasing chain length. The two runs shown in Figure 4 indicate the relatively minor effect that the C_{14} and C_{12} alcohols have on mass transfer. Figures 5 and 6 present experimental results indicating that as the surface pressure of the C_8, C_6, and C_4 alcohols is increased, the mass transfer enhancement increases. In Figure 7, the effect of the C_{18}, C_{14}, and C_6 amide is shown to be quite small. As the chain length of the amines in Figure 8 is decreased from twenty-two to eighteen to fourteen, the mass transfer reduction is decreased. The six-carbon amine in Figure 8 exhibits somewhat different behaviour from the alcohols in that the highest surface pressure run resulted in less mass transfer enhancement than two lower surface pressure runs.

The model for absorption with the monolayer present is complex. Several investigators (*23*, *26*) have used the surface resistance boundary condition to describe the effect of surface active agents in retarding mass transfer. This interfacial boundary condition as applied to the mathematical model, Equations (3), (4), and (5), is

$$-D^E \left(\frac{\partial C^B}{\partial \xi}\right)_{\xi=0} = k_s \left[C^{B*}(t) - C^B(\xi = 0, t)\right] \tag{13}$$

Unfortunately, an analytical solution of Equation (3) subject to (*4a*), (*4b*), Equation (13) as boundary condition 2, and (5) could not be obtained; therefore, the following approach was employed. Vrentas (*40*) has shown that the interfacial concentration $C_i^B(t)$ may be expressed as a function of the interfacial mass transfer N_ξ:

$$C_i^B(t) = C_0 + \frac{2}{\sqrt{\pi D^E}} \int_0^{\sqrt{t}} N_\xi \left(\xi = 0, t - q^2\right) dq \tag{14}$$

For this study

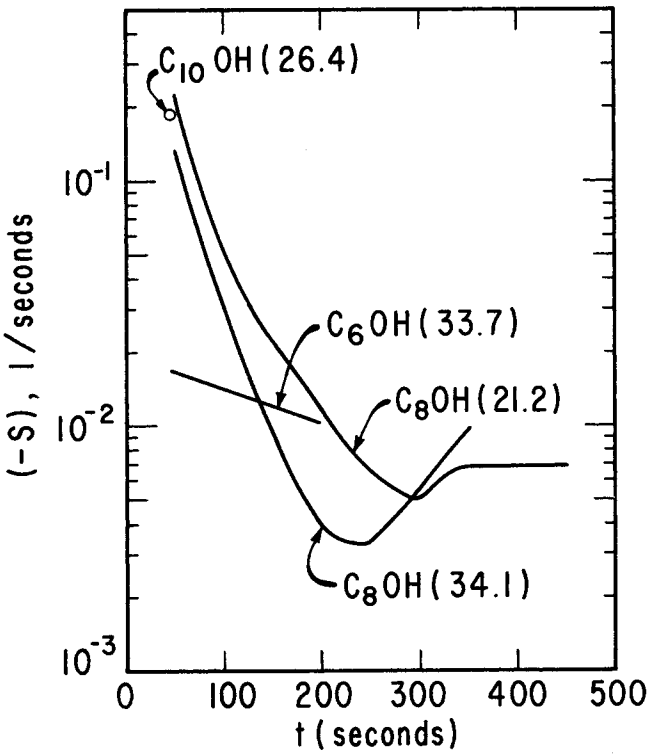

Fig. 11. Surface renewal coefficient vs. time for C_{10}, C_8, and C_6 alcohol. (Surface pressure in dynes/cm. in parentheses.)

$$N_\xi(\xi = 0, t) = -\frac{H_1}{K}\frac{dp}{dt} \qquad (15)$$

If Equation (15) is used to compute the interfacial mass transfer for runs with pure water, the interfacial concentration $(C_i^B)_W$, where the subscript W indicates that pure water is being considered, may be computed from Equation (14). Values of $(C_i^B)_W$ should be obtained which would be equal to the concentration of ammonia in the interface in equilibrium with the pressure of ammonia at the given time, because equilibrium was assumed between the gas and liquid phase.

A measure of the fit of the absorption data in pure water is to determine if Δ_W is essentially zero, where Δ_W is defined as

$$\Delta_W = (C^* + H_1 p + H_2 p^2)_W - (C_i^B)_W \qquad (16)$$

For the case of surface active agents which retard mass transfer, the interfacial concentration of ammonia in the liquid is not in equilibrium with the gas-phase pressure of ammonia. There is a concentration driving force Δ_{SAA} across the interface, which can be defined by

$$\Delta_{SAA} = (C^* + H_1 p + H_2 p^2)_{SAA} - (C_i^B)_{SAA} \qquad (17)$$

where the subscript SAA indicates that the chamber containing the surface active agent is being considered. The concentration of ammonia in the interface $(C_i^B)_{SAA}$ was computed from Equations (14) and (15) by using the experimental pressure data for the chamber with the surface active agent. The surface mass transfer coefficient k_s was defined as

$$k_s = \frac{[N_\xi(\xi = 0, t)]_{SAA}}{\Delta_{SAA} - \Delta_W} \qquad (18)$$

The concentration driving force $\Delta_{SAA} - \Delta_W$ was used instead of Δ_{SAA} alone in order to correct for the numerical integration errors in the determination of Δ_{SAA} and Δ_W. Those values of k_s obtained at the initial times for those surface active agents that retarded mass transfer to a small extent were the only ones affected by this change.

Values of the surface mass transfer coefficient k_s for the nine compounds that retarded the mass transfer of ammonia into water are presented in Figures 9 and 10 as functions of time. The runs with the largest values of the surface mass transfer coefficient were the runs in which mass transfer was retarded the least.

For the surface active agents which were found to increase mass transfer rates, movements in the interface were observed. Therefore, the possibility of modeling the process by the surface renewal concept was investigated. The mathematical model developed here is an extension of Danckwerts' work (*16*). He proposed a surface age distribution curve as follows:

$$\phi(\theta) = \frac{Se^{-S\theta}}{1 - e^{-St}}, \qquad 0 \leq \theta \leq t \qquad (19)$$

Once a surface age distribution curve is obtained, one may compute the flux of ammonia into a surface by

$$N_\phi(t) = \int_0^t \phi(\theta) N_\xi(\xi = 0, \theta)\, d\theta \qquad (20)$$

A complicating factor in extending the surface renewal model, given by Equation (20), to this system is that the pressure of ammonia is continually changing with time. Consider an element of the surface which was formed at a contact time of $t - \theta$. At contact time t, the surface age of this element is $t - (t - \theta)$ or θ. At $t - \theta$, the pressure of ammonia is different from the pressure at other times; therefore, the instantaneous flux depends on the pressure of ammonia at the time $(t - \theta)$ a new element of surface was formed as well as the surface age, θ, of that element.

For the purposes of the mathematical model given by Equation (20), the instantaneous flux was computed as follows:

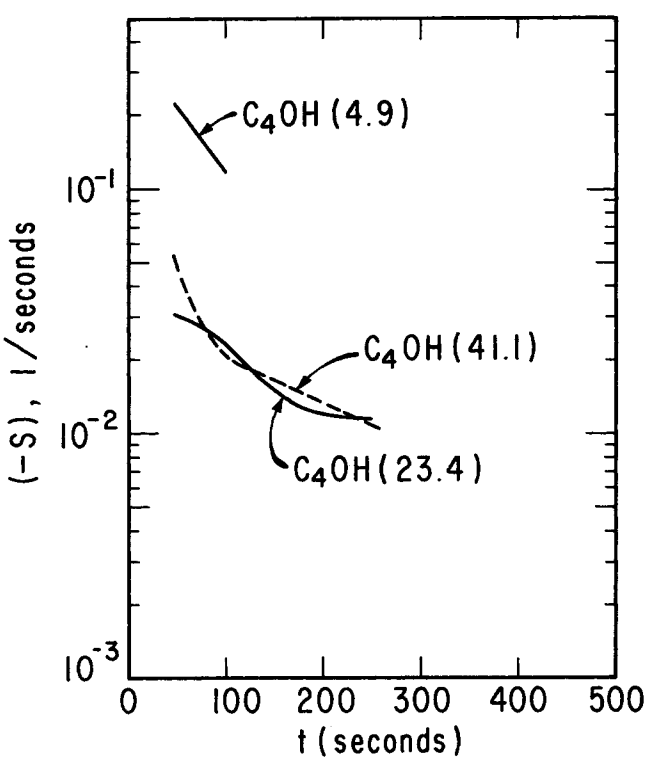

Fig. 12. Surface renewal coefficient vs. time for C_4 alcohol. (Surface pressure in dynes/cm. in parentheses.)

$$N_\xi(\xi = 0, \theta) = -\frac{H_1}{K}\frac{dp}{d\theta} = -\frac{H_1}{K}\sum_{j=1}^{\infty} a_j \theta^{\frac{j}{2}-1}\left(\frac{j}{2}\right) \tag{21}$$

The a_j depend on the appropriate initial ammonia pressure (which shall be called π_0), C^*, H_1, H_2, K, D^E, and C_0. The symbol π_0 is used here in the absorption of ammonia by water containing a surface active agent to indicate the ammonia pressure at a contact time of $t - \theta$. If the experimentally determined ammonia pressure for absorption by water containing a surface active agent is indicated by $p_{SAA}(t)$, then

$$\pi_0 = p_{SAA}(t - \theta) \tag{22}$$

Equation (19) was used to compute the surface age distribution function, and Equations (21) and (22) were used to calculate the flux distribution function. These functions were then introduced into Equation (20), which was numerically integrated to determine the integrated flux $N_\phi(t)$. The value of S which gave an integrated flux $N_\phi(t)$ equal to the experimentally determined flux was determined by Newton's method.

Values of the surface renewal coefficient $(-S)$ for the seven compounds that increased the mass transfer of ammonia into water are presented in Figures 11, 12, and 13 as functions of time. As the quantity $(-S)$ became large, the surface renewal model predicted fluxes that were closer to the flux of ammonia into pure water. Therefore, the runs with large values of the quantity $(-S)$ increased mass transfer less than the runs with small values of $(-S)$.

It was informative to correlate the surface mass transfer coefficient with the molecular properties of the surface active agent. Correlations of this type permit the prediction of the effect of other surface active agents that have similar molecular properties.

Since the surface mass transfer coefficient varies with time, some statistic of the surface mass transfer coefficient vs. time curve must be selected for purposes of correlation. The curves of Figure 9 and 10 were averaged to obtain a time average surface mass transfer coefficient $\overline{k_s}$ by the formula

$$\overline{k_s} = \frac{1}{t}\int_0^t k_s\, dt \tag{23}$$

Figure 14 presents the correlation which was determined

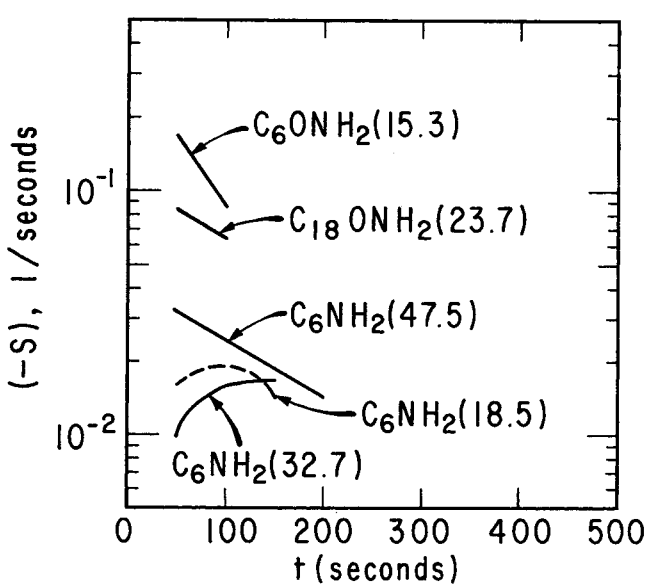

Fig. 13. Surface renewal coefficient vs. time for C_{18} and C_{16} amide and C_6 amine. (Surface pressure in dynes/cm. in parentheses.)

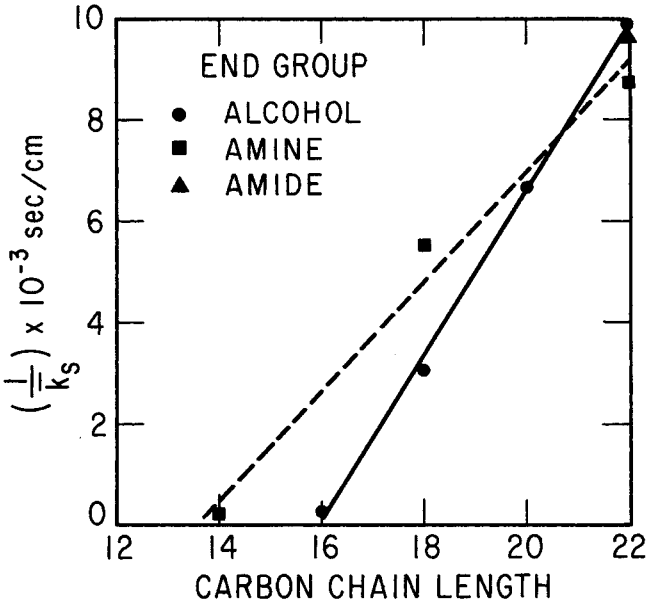

Fig. 14. Correlation of $\left(\frac{1}{\overline{K_s}}\right)$ with carbon chain length with parameter of varying end group.

for the average surface mass transfer coefficient as a function of chain length. The reciprocal of the average surface mass transfer coefficient $1/(\overline{k_s})$ (also known as the *surface resistance*) for the surface active agents of a given end group appeared to be approximately a linear function of the hydrocarbon chain length.

CONCLUSIONS

Perhaps the most interesting result of this study was the discovery that the addition of certain soluble surface active agents to a water phase increased the absorption of ammonia into that aqueous phase. It is believed that the movement which was detected in the interface of these solutions was caused by the Marangoni effect, that is, the generation of movement in an interface by longitudinal variations of interfacial tension. Sternling and Scriven (38) have treated the Marangoni effect extensively.

A point of interest is why there was no observable instability in the case of the insoluble films. One reasonable explanation is that rigid surface films do not have surface tension gradients. Another explanation is that even with surface tension gradients, the rigid insoluble films stabilize the surface by preventing convection.

From inspection of the experimental data of this study, several general rules of behavior for the surface active agents in question could be deduced.

1. For insoluble films with a given end group and surface concentration, the retardation of mass transfer increased as the chain length of the film increased.
2. For insoluble films with a given surface concentration, the effect of various end groups depended on the length of the carbon chain in question. For an eighteen-carbon chain, the retardation effect was alcohol > amine > amide. For very long carbon chains (twenty-two carbon atoms), the end group only had a small influence on the retardation effect.
3. In general, for solutions of soluble surface active agents at a given surface pressure and for a given end group, the mass transfer enhancement increased as the chain length decreased.
4. For a given soluble surface active agent, as the sur-

face pressure decreased from its maximum value, the mass transfer enhancement could initially increase but ultimately decreased.

5. For solutions of soluble surface active agents at a given surface pressure and hydrocarbon chain length, the end group effect on mass transfer enhancement was amine > alcohol > amide.

ACKNOWLEDGMENT

Gratitude is expressed to the National Science Foundation for the fellowship granted during this investigation and to the U. S. Public Health Service for the grant (WP 00652) which supported this research.

NOTATION

A = area for mass transfer
a_j = j^{th} coefficient in the power series expansion
C^B = molal concentration of solute gas
C^{B*} = molal concentration of solute gas in equilibrium with the gas phase
C_i^B = interfacial liquid concentration in molal units
C^V = g. moles of water/liter of ammonia solution
C^W = g. mole of water/liter of water, a constant
C_0 = initial molal concentration of solute gas
C^*, H_1, H_2 = constants used to fit equilibrium liquid concentration in molal units to a quadratic function of p
D = molecular diffusion coefficient in the x system
D^B = molecular diffusion coefficient in ξ system
D^E = effective diffusion coefficient in ξ system
J_ξ = ξ component of the diffusional flux vector in the ξ coordinate system
K = collection of constants, $(A H_1)/(V \delta)$
k_s = surface mass transfer coefficient
$\bar{k}_s$ = average surface mass transfer coefficient
N_ξ = ξ component of molar flux in ξ coordinate system
N^T = total molar flux of solute gas and water
p = gas-phase ammonia pressure
p_0 = initial gas-phase ammonia pressure
p_{SAA} = ammonia pressure in compartment with the surface active agent
p_W = ammonia pressure in compartment with pure water
q = dummy variable
S = surface renewal coefficient
S_{50} = surface renewal coefficient at $t = 50$ sec.
S_p = deviation of experimental pressure from calculated pressure
t = contact time since system pressurization ended
V = gas-phase volume
V_W = volume of 1 g. mole of water, a constant
v_ξ = ξ component of the molar average velocity in the ξ coordinate system

Greek Letters

Δ_p = differential pressure between compartments
Δ_{SAA} = concentration driving force across the interface of water containing a surface active agent
Δ_W = concentration driving force across the interface of pure water
δ = constant which converts pressure to concentration
θ = surface age
ξ = special coordinate
π_0 = initial pressure in the surface renewal model
ϕ = surface age distribution function

Subscripts

SAA = surface active agent
W = water without a surface active agent

LITERATURE CITED

1. Aiba, S., and K. Toda, *J. Gen. Appl. Microbiol.*, **9**, 443 (1963).
2. Anthony, R., and D. M. Himmelblau, *J. Phys. Chem.*, **67**, 1080 (1963).
3. Baird, M. H. I., and J. F. Davidson, *Chem. Eng. Sci.*, **17**, 87 (1962).
4. Blank, M., "Retardation of Evaporation by Monolayers," p. 75, Academic Press, New York (1962).
5. ———, and F. J. W. Roughton, *Trans. Faraday Soc.*, **56**, 1832 (1960).
6. Burnett, J. C., Ph.D. dissertation, Univ. Tex., Austin (1966).
7. Burrows, G., and F. H. Preece, *Trans. Inst. Chem. Engrs. (London)*, **32**, 99 (1954).
8. Carslaw, H. S., and J. C. Jaeger, "Conduction of Heat in Solids," 2 ed., p. 483, Oxford, London, England (1959).
9. Carver, C. E., "Biological Treatment of Sewage and Industrial Wastes," p. 149, Reinhold, New York (1956).
10. Chiang, S. H., paper presented at Am. Inst. Chem. Engrs. Annual Meeting, Philadelphia, Pa. (Dec., 1965).
11. ———, and H. L. Toor, *AIChE J.*, **10**, 398 (1964).
12. Chu, J. C., C. C. Taylor, and D. J. Levy, *Ind. Eng. Chem.*, **42**, 1157 (1950).
13. *Ibid.*, p. 221.
14. Cullen, E. J., and J. F. Davidson, *Chem. Eng. Sci.*, **6**, 49 (1956).
15. ————————, *Trans. Faraday Soc.*, **53**, 113 (1957).
16. Danckwerts, P. V., *Ind. Eng. Chem.*, **43**, 1460 (1951).
17. Davies, J. T., A. A. Kilner, and G. A. Ratcliff, *Chem. Eng. Sci.*, 19, 583 (1964).
18. Eckenfelder, W. W., and E. L. Barnhart, *AIChE J.*, **7**, 631 (1961).
19. Emmert, R. E., and R. L. Pigford, *Chem. Eng. Progr.*, **50**, 87 (1954).
20. Goodridge, F., and D. J. Bricknell, *Trans. Inst. Chem. Engrs. (London)*, **40**, 54 (1962).
21. Griffith, R. M., *Chem. Eng. Sci.*, 13, 198 (1960).
22. Hartley, G. S., and J. Crank, *Trans. Faraday Soc.*, **45**, 801 (1949).
23. Harvey, E. A., and W. Smith, *Chem. Eng. Sci.*, **10**, 274 (1959).
24. Hawke, J. G., *Proc. Austr. Atomic Energy Symp.*, 634 (1958).
25. ———, and A. E. Alexander, "Retardation of Evaporation by Monolayers," p. 67, Academic Press, New York (1962).
26. Hawke, J. G., and A. G. Parts, *J. Coll. Sci.*, **19**, 448 (1964).
27. Hawke, J. G., and I. White, *J. Phys. Chem.*, **70**, 3369 (1966).
28. Hawke, J. G., and H. J. L. Wright, *Nature*, **212**, 810 (1966).
29. Higbie, Ralph, *Trans. Am. Inst. Chem. Engrs.*, **31**, 365 (1935).
30. La Mer, Victor K., "Retardation of Evaporation by Monolayers," Academic Press, New York (1962).
31. Linton, M., and K. L. Sutherland, *Austral. J. Appl. Sci.*, **9**, 18 (1958).
32. Lynn, S., J. R. Straatemeir, and H. Kramers, *Chem. Eng. Sci.*, **4**, 49 (1955).
33. Mancy, K. H., and D. A. Okun, *J. Water Pollution Control Federation*, **32**, 351 (1960).
34. Mirev, D., D. Elenkov, and C. Balarev, *Compt. Rend. Acad. Bulgare Sci.*, **14**, 349 (1961).
35. Plevan, R. E., Ph.D. thesis, Univ. Ill., Urbana (1965).
36. Raimondi, Pietro, and H. L. Toor, *AIChE J.*, **5**, 86 (1959).
37. Sada, Eizo, and D. M. Himmelblau, *ibid.*, **13**, 860 (1967).
38. Sternling, C. V., and L. E. Scriven, *ibid.*, **5**, 515 (1959).
39. Timson, W. J., and C. G. Dunn, *Ind. Eng. Chem.*, **52**, 799 (1960).
40. Vrentas, J. S., Ph.D. thesis, Univ. Del., Newark (1963).
41. Zieminski, S. A., C. C. Goodwin, and R. L. Hill, *Tappi*, **43**, 1029 (1960).
42. Zieminski, S. A., and R. L. Hill, *J. Chem. Eng. Data*, **7**, 51 (1962).

Manuscript received April 18, 1968; revision received August 16, 1968; paper accepted August 21, 1968.